Two distinct systems represent contralateral and ipsilateral sensorimotor processes in the human premotor cortex: A dense Transcranial Magnetic Stimulation (TMS) mapping study

Carlotta Lega[1], Leonardo Chelazzi[1,2], Luigi Cattaneo[1,2*]

[1] Department of Neuroscience, Biomedicine and Movement, University of Verona, Italy

[2] Italian Institute of Neuroscience (INN), Verona, Italy

*Corresponding author:

Luigi Cattaneo

Department of Neuroscience, Biomedicine and Movement Sciences,

Section of Physiology and Psychology, University of Verona,

Strada Le Grazie 8, 37134 Verona, ITALY

luigi.cattaneo@univr.it

ABSTRACT

Animal brains contain behaviorally-committed representations of the surrounding world, which integrate sensory and motor information. In primates, sensorimotor mechanisms reside in part in the premotor cortex (PM), where sensorimotor neurons are topographically clustered according to functional specialization. Detailed functional cartography of the human PM is still under investigation. We explored the topographic distribution of spatially-dependent sensorimotor functions in healthy volunteers performing left or right, hand or foot, responses to visual cues presented in the left or right hemi-space, thus combining independently stimulus side, effector side and effector type. Event-related Transcranial Magnetic Stimulation was applied to single spots of a dense grid of 10 points on the participants' left hemi-scalp, covering the whole PM. Results showed: a) spatially segregated hand and foot representations; b) focal representations of contralateral cues and movements in the dorsal PM and c) distributed representations of ipsilateral cues and movements in the ventral, and dorso-medial PM. The present novel causal information indicates that: a) the human PM is somatotopically organized and b) the left PM contains sensory-motor representations of both hemispaces and of both hemibodies, but the hemispace and hemibody contralateral to the PM are mapped on a distinct, non-overlapping cortical region compared to the ipsilateral ones.

KEYWORDS: voluntary movement; brain mapping; motor cortex; somatotopy, bilateral motor representation.

INTRODUCTION

In everyday life, we constantly use cues from the space around us to perform appropriate actions. Our current knowledge of the neural processes underlying visuomotor behavior is founded on solid neurophysiological evidence from the macaque model. In non-human primates, as a rule, behaviorally-relevant visual information is transformed into a body-centered coordinate system along the dorsal visual stream and promptly transferred to the premotor cortex (PM) where it is mapped onto goal-oriented motor patterns (Rizzolatti and Luppino 2001; Cisek and Kalaska 2010; Caminiti et al. 2015; Borra et al. 2017). The parietal and premotor cortices are the main site of sensorimotor integration, where overlapping populations of neurons show alternatively purely sensory, sensorimotor or purely motor properties. The parieto-premotor system is anatomically and functionally heterogeneous: cytoarchitectonic findings indicate a series of different sub-regions (Geyer et al. 2000) that are interconnected by mainly parallel white matter bundles within the superior longitudinal fascicle. Local functional specializations are defined according to the sensory and motor properties of the corresponding neurons. A well-accepted organizational principle of the neural substrates of upper limb movements divides the primate parietal cortex in a medial and a lateral system, which are dubbed dorso-medial and dorso-lateral systems, on account of being both embedded in the dorsal visual stream (Rizzolatti and Matelli 2003; Caminiti et al. 2015; Gallivan and Culham 2015; Borra et al. 2017; Monaco et al. 2017). Anatomically, the dorso-medial pathway connects the posterior parietal cortex (PPC) with the dorsal premotor cortex (dPM, Caminiti et al. 1991), whereas the dorso-lateral system connects the anterior part of the intraparietal sulcus (AIP) and area F5 within the ventral premotor cortex (vPM, Rizzolatti et al. 1988; Murata et al. 1997; Fluet et al. 2010). Neurons with spatial properties are predominant in the dorso-medial system and are necessary for spatially-oriented behavior; neurons in the dorso-lateral system are tuned to objects' invariant geometrical features and are

necessary for grasping behavior (Jeannerod et al. 1995; Brochier and Umiltà 2007; Fluet et al. 2010; Bonini et al. 2012; Schaffelhofer and Scherberger 2016; Borra et al. 2017). Importantly, this classical model has been shown to be incomplete and recent findings in non-human primate called into question the ventral vs. dorsal strict dichotomy in the parieto-frontal circuits (Raos et al. 2004; Fattori et al. 2010; Vargas-Irwin et al. 2015; Lanzilotto et al. 2016; Papadourakis and Raos 2018; Livi et al. 2019). With respect to object processing for grasping, many recent investigations described relevant neural activity in the parieto-frontal dorso-medial system (Raos et al. 2004; Fattori et al. 2010; Vargas-Irwin et al. 2015; Lanzilotto et al. 2016; Papadourakis and Raos 2018; Livi et al. 2019). Similarly, spatially-oriented representation of reaching-grasping behaviours has been described in the lateral pathway (Lehmann and Scherberger 2013, 2015; Bonini et al. 2014). In light of this evidence, recently some authors proposed to extend the classical object-grasping network, by including the anterior subdivision of ventral area F5-sub-area F5a-, and the pre-supplementary area (area F6), (Lanzilotto et al. 2016; see Bonini 2017; Gerbella et al. 2017). Furthermore, tracing studies directly show that the dorso-medial and dorso-lateral pathways are not completely anatomically segregated (e.g. Gharbawie et al. 2011; Janssen et al. 2018; Livi et al. 2019). In accordance with monkey literature (Murata et al. 1997; Baumann et al. 2009; Fattori et al. 2010, 2012; Fluet et al. 2010; Lanzilotto et al. 2016; Gerbella et al. 2017), also evidence in human did not support a rigid functional dissociation (Gallivan, McLean, Valyear, et al. 2011; Verhagen et al. 2012; Gallivan et al. 2013; Fabbri et al. 2014; Monaco et al. 2015; Turella et al. 2016), suggesting that both pathways could code for grasping information. Accordingly, neuroimaging studies demonstrated that both visually-guided (Gallivan, McLean, Valyear, et al. 2011; Gallivan et al. 2013) and non-visually-guided (Fabbri et al. 2014) reach-to-grasp actions activated not only the vPM, but also a more dorsal part of the premotor cortex.

The granularity of sensory and motor representations in the premotor cortex is coarse. The issue of possible bilateral representations of the upper limb in the premotor cortex of macaque monkeys is complex and somehow depends on what meaning we attribute to the term “neural representation”. Intracortical microstimulation (ICMS) of the premotor cortex produces only contralateral movements in the convexity of the hemisphere (ventral and dorsal sectors of the PM), whereas ICMS (Mitz and Wise 1987; Luppino et al. 1991) of the medial PM evokes bilateral movements. The PM is defined by a higher stimulation threshold than M1 (Weinrich and Wise 1982) and it is generally accepted that excitability is correlated with the existence of corticospinal connections. Therefore, ICMS-based mapping of motor function is reductive, being restricted to regions giving rise to corticospinal projections. In alternative to ICMS, longer stimulation protocols with higher stimulus intensities have shown much larger maps, with full bilateral upper limb movements from the dorsal premotor cortex, but only contralateral movements after stimulation of the ventral premotor cortex (see Graziano 2009 for a review). A different picture emerges from single-unit recordings in awake monkeys. Premotor neurons fire predominantly in association with contralateral upper limb movements, but a large percentage of them fire also when monkeys perform contralateral movements. In fact, coding bilateral movements in the pre-movement period is the most frequent pattern in dorsal premotor and medial premotor neurons (Tanji et al. 1988; Kermadi et al. 2000; Cisek et al. 2003; Ganguly et al. 2009) and even in restricted portions of M1 (Aizawa et al. 1990; Donchin et al. 1998). Oddly enough, the same studies report a small but significant percentage of neurons in the PM that fire in conjunction with ipsilateral movements only. In the ventral PM the picture is less clear and the limited data indicate that PM contains neurons that either code contralateral movements or code indifferently the visual features of a target, independently of the effector to be used, but no strictly “ipsilateral” neurons have been

found (Gentilucci et al. 1988; Rizzolatti et al. 1988; Hoshi and Tanji 2006). Sensory receptive fields in the PM are very large (Rizzolatti et al. 1981), sometimes including the whole visual field.

The biomechanical and evolutionary similarities between human and non-human primates allowed to exploit the monkey as a model to deepen our mechanistic understanding of the human brain's "action system" (Rizzolatti et al. 2014; Caminiti et al. 2015). Human data lack the single-cell resolution level, and are mostly collected with non-invasive techniques, an experimental approach that poses several methodological problems in the study of voluntary movement. At the same time, functional neuroimaging lacks the temporal resolution to investigate the neural correlates of unfolding movements. Indeed, most fMRI studies on voluntary actions focus on the preparatory phase prior to the actual movement (Medendorp et al. 2005; Beurze et al. 2007, 2009). Transcranial magnetic stimulation (TMS) does not suffer from these limitations and has been successfully applied to the human cortex during actual movement and during fast visuomotor integration prior to it. Several TMS studies (Schluter et al. 1998, 2001; Johansen-Berg et al. 2002; Koch, Franca, Fernandez Del Olmo, et al. 2006; O'Shea et al. 2007; Bardi et al. 2015) demonstrated that the PM is required for externally-triggered action selection, with a dominant role of the left hemisphere (Schluter et al. 1998, 2001; Johansen-Berg et al. 2002; Koch, Franca, Fernandez Del Olmo, et al. 2006; Bardi et al. 2015). Indeed, TMS of PMd on either side disrupts response selection with the contralateral hand, but only left PMd TMS disrupts selection with the ipsilateral hand (Schluter et al. 1998, 2001; Johansen-Berg et al. 2002; Koch, Franca, Fernandez Del Olmo, et al. 2006; O'Shea et al. 2007). Sensory properties of the PM have been less frequently the object of ad-hoc investigation with TMS because studies on visuomotor behavior commonly employ visual stimuli in central vision. Moreover, TMS studies generally explore a single cortical target that was chosen a priori within the PM, therefore they yielded limited spatial information on the overall functional organization of the PM region. Instead, dense mapping with TMS, i.e. stimulating the cortex across a uniform array of

adjacent target-foci, allows the detailed cartography of circumscribed cortical regions (Busan et al. 2009; Stoeckel et al. 2009; Cattaneo and Barchiesi 2011; Maule et al. 2015; Cattaneo 2018).

The main aim of the present work is to describe, in the healthy human's whole PM, the cortical topography of spatially-defined sensorimotor representations, investigating separately the ipsilateral and contralateral space for both visual cues and body movements. Specifically, we wanted to determine the functional properties of this brain region in terms of spatial specificity and of effector specificity. In light of previous studies suggesting an effector-specific organization of parietal and premotor regions (Heed et al. 2016), we required participants to produce responses with hands or feet in different blocks. This allowed us to explore the anatomical distribution of the motor representation of two different effectors: the upper and the lower limb. To this aim, we applied TMS over the left PM, which in turn allowed us to describe, in the healthy human's whole PM, where are the ipsilateral and contralateral visual space and the ipsilateral and contralateral body movements represented. For the sake of clarity, in this specific context, we will refer to the term "ipsilateral" to indicate left movement and left visual space (that is ipsilateral to left PM stimulation) and to the term "contralateral" to indicate right movement and right visual space. To draw a functional cartography of the PM, we used a dense-transcranial magnetic stimulation (d-TMS) mapping technique that allows to probe the cortical surface without having to rely on strict a-priory hypotheses on where to stimulate to produce a given behavioral effect. This in turn allows to generate spatially unbiased data and to reduce significantly spatial noise due to anatomical variability across subjects (Cattaneo 2018). We applied event-related TMS to a grid of 10 points covering the whole of the left PM in healthy voluntary participants, while they performed a spatial task. We chose the so-called Simon task (Simon and Rudell 1967), a classical spatial-motor task from experimental psychology, that enables to explore the dimensions of effector side and visual stimulus side independently, in an orthogonal factorial 2x2 (effector side x

stimulus side) design. An additional advantage of the Simon task is that spatial information is not explicitly present in the instructions and is task-irrelevant. Movements are instructed by means of a symbolic cue (the target color), thus avoiding any effect of semantic/verbal material on motor performance. Following the classification of sensorimotor transformation formulated by Lebedev and Wise (2002), the Simon task belongs to what the authors called “arbitrary nonstandard mapping”, in which the location of the stimulus is irrelevant and its other features (i.e. the color) guide the movement (Wise et al. 1996). In this framework, it is important to note the difference with “standard sensorimotor mappings”, where instead the object is also the target to be approached and directly guides the corresponding action. In this sense, contrary to “arbitrary nonstandard mapping”, there is a direct (vs. indirect) mapping between vision and action. Two other features of the Simon task on which we capitalized in the present experimental design are 1) the possibility of performing responses with effectors other than the upper limb (in our case the foot) and 2) the added value of assessing sensorimotor associations with different levels of complexity in terms of dimensional overlap. Same-side stimulus-response associations (known as compatible stimulus-response associations) are considered sensorimotor mappings with overlapping spatial features, while opposite-side stimulus-response associations are considered non-overlapping and are performed at a cost in performance (Kornblum et al. 1990; Hasbroucq and Guiard 1991).

The results first indicated that hand and foot movements were represented in non-overlapping regions of the PM, with foot actions represented more dorsally and caudally compared to hand actions. In upper limb trials, right-sided (contralateral) visual stimuli and movements were modulated by TMS applied to a single region in the mid-dorsal PM. Left (ipsilateral) visual stimuli and movements were modulated by TMS applied to two different PM foci: a central-anterior locus in the dorsal PM and one in the ventral PM. On the contrary, the

effect of stimulus-response compatibility did not differ between the sham and the active TMS stimulation at any site. We conclude that the human left PM does indeed contain a full representation of both visual hemispaces and of bodily movements involving the upper and lower extremities bilaterally, but contralateral and ipsilateral features are supported by two distinct, only partially overlapping cortical networks.

METHODS

Participants

Sixteen participants took part in the experiment (11 F, mean age = 22.72, SD = 1.98, range = 19-27). All participants were right-handed (Oldfield 1971). Prior to the TMS experiment, each subject filled in a questionnaire to evaluate compatibility with TMS. None of the participants reported neurological problems, history of seizure and did not present any contraindications related to the use of transcranial magnetic stimulation (Rossi et al. 2009). Written informed consent was obtained from all participants before the experiment. The protocol was approved by the local ethical committee and participants were treated in accordance with the Declaration of Helsinki.

General protocol

The experiment was organized in repeated trials, according to a factorial design that included factors inherent to TMS (locus of application) and the behavioral task (effector, side of visual stimulus, side of response). In each trial, participants completed the behavioral task and were stimulated by effective or sham TMS in an event-related way. Effective TMS was applied to a specific location within a grid of 10 points (one point for every trial) covering the whole of the left premotor cortex in each subject. The experimental measure of interest was the response time, or

the time interval between appearance of the visual stimulus and the behavioral response (see below). Data analysis was performed by means of a statistical parametric mapping approach. We built individual maps of t-statistics parameters for each participant by comparing trials with real TMS with those with sham TMS, grouped according to behavioral factors of interest (for example hand responses vs. foot responses). Finally, between-subject point-by-point comparisons (using paired t-tests) between t-statistical maps were performed to obtain group-level premotor statistical maps.

Procedure

Participants were sitting on a chair, with the head on a chin-rest, facing a LCD computer screen. They were required to make a right vs. left manual or pedal response depending on the color of the visual stimulus, a square shape, presented on either side of the screen. The target stimulus was either a green (RGB color co-ordinates: 134, 148, 0; luminance: 15.7 cd/m2) or red (246, 0, 0; 15.6 cd/m2) square subtending 4°× 4° (width × height) of visual angle presented on a white background. Each participant was tested in two identical experimental sessions lasting 2 h each. The timeline of an experimental trial is shown in Figure 1. Each trial started with the presentation of a central fixation cross lasting 1000 msec. Then a stimulus was presented at a visual angle of 8° either to the left or to the right of the central fixation point until participants' response. The inter-trial interval was 4000 msec. No feedback on performance was provided. Participants were instructed to maintain their gaze on the fixation point during the whole experimental session. Participants had to respond with either hands or feet in separate blocks. In the hand-block participants were required to position the right and left index finger on two response buttons positioned to the right and to the left of the body midline, respectively. Similarly, in the foot-block they were required to position the right and the left feet on two pedals

respectively positioned to the right and to the left of the body midline. Response buttons and pedals were aligned in space with the visual stimuli. The whole experiment was performed alternating hand and foot response blocks with half of the participants starting with the hand block and the other half with the foot block. Half of the participants were instructed to press the right response button (or right pedal) with the right index finger/right foot when the target square was red and the left response button with their left index finger/left foot when the target square was green (Figure 1). The other half of the participants received the opposite hand/foot-target assignment. Both speed and accuracy were emphasized. The whole experiment was divided into thirty-two experimental blocks. Sixteen blocks were administered on a first day (eight with hand-response and eight with foot-response), the other sixteen on a second day. Each block was composed of 52 trials in which stimulus position (left or right), response side (left or right) and TMS site (13 sites of stimulation, 10 active sites + 3 sham sites) were fully crossed to produce the same number of trials for each possible combination, presented in a random order. The software Open-Sesame (Mathôt et al. 2012) was used for stimuli presentation, data collection and TMS triggering.

TMS mapping procedure

A schematic visualization of the thirteen stimulated sites is shown in Figure 2. For each participant, we built a 13–point grid drawn over the left PM (Brodmann's area 6). The localization of the premotor cortex was based on probabilistic cytoarchitectonic atlases (Zilles et al. 2002; Amunts et al. 2007; Zilles and Amunts 2010; Mohlberg et al. 2012). Stimulation targets were placed equidistant from one another, with a 2 cm inter-target distance. The grid was determined by referencing to the individual motor hand area, motor foot area and motor lip area, which corresponded to the 3 control sham points. The grid was determined as follows: Firstly, we

identified the three sham points, corresponding to the three hotspots where single pulse TMS induced a visible muscle twitch in the contralateral hand, contralateral foot and lip, respectively. Then, starting from the first sham point (foot motor area) we moved anteriorly 2 cm by 2 cm, identifying points 1, 2 and 3. With the same procedure we identified two points anteriorly to the motor hand area (point 7 and 8) and one single point 2 cm anterior to the lip motor area (point 10). Point 4 and 5 corresponded to the points half-way between points 1-7 and between points 2-8, respectively. Moving 2 cm forward relative to point 5, we identified point 6. Finally, point 9 was identified half-way between points 7-10. A scalp marking was made on each subject over each location. For illustration purpose in Figure 2 we represented on a surface of the colin27 brain template the 10-point grid over the left premotor cortex (Brodmann's area 6) and the corresponding 3 sham points along the primary motor cortex. The location of the premotor cortex is indicated as a probabilistic map (source: , the JuBrain Cytoarchitectonic Atlas, available at: https://www.jubrain.fz-juelich.de/apps/cytoviewer/cytoviewer-main.php#).

Transcranial Magnetic Stimulation

Dual-pulses TMS (10Hz) was delivered starting 50 ms after the stimulus onset. A 70-mm figure-of-eight stimulation coil was placed over the stimulation sites tangentially to the skull, with the handle pointing backward at a 45° angle from the midsagittal line. For the three sham points the coil was held at a 90° position to ensure that the magnetic field did not stimulate the target area. Indeed, this sham condition has been proven to be ineffective in producing an electric field capable of changing neuronal excitability (Lisanby et al. 2001). TMS was applied with a Magstim Super Rapid2 system (Magstim Company, Whitland, UK). The intensity of the magnetic stimulation was set separately for each participant 10% above the individual motor threshold and was kept constant between sessions. We checked in each participant whether stimulation over the defined

10 premotor sites evoked any MEPs and we moved the coil 0.5 cm anterior if this was the case, re-assessing the grid spots, accordingly. The rMT was determined using the software based "adaptive method" developed by (Awiszus, 2003) (Motor Threshold Assessment Tool, version 2.0: http://www.clinicalresearcher.org/software.htm). A MEP ≥ 50 μV peak-to-peak amplitude was fed back to the software as valid response. MEPs were recorded by using 10-mm Ag/AgCl surface cup electrodes. The active electrode was placed over the FDI muscle of the right hand and the reference electrode over the metacarpo-phalangeal joint of the index finger. The electromyographic signal was sampled and amplified by using a Digitimer D360 amplifier (Digitimer Ltd, Welwyn Garden City, UK) through filters set at 20 Hz and 2 kHz with a sampling rate of 5 kHz, digitized by an analog-digital converter (Power 1401, Cambridge Electronic Design Cambridge, UK) and then stored using the Signal software (Cambridge Electronic Design, Cambridge, UK). The mean stimulating intensity was 58% of the maximum stimulator output.

Data analysis

The analysis was carried out with the MATLAB software. The complete scripts for data analysis are available online on 'https://osf.io/t6cp9/' , stored on the Open Science Framework data sharing platform (Foster and Deardorff 2017). The analysis was performed on response times (RTs) and followed a series of steps.

Pre-processing steps: A) Identification of a comparison of interest (for example responses given with the right-hand vs. responses given with the left hand or responses given for the right stimulus vs. responses given for the left stimulus) and grouping of trials according to the comparison of interest and to the site of stimulation. In this way each subject was characterized by 26 sets of trials according to a multifactorial design having as factors: conditions of interest (2 levels, for example left vs right hand) x spots (13 levels: 10 active spots + 3 sham spots) design; B)

Comparisons across the 3 sham spots within condition and subsequent collapse of the sham data into a single value. In this way each subject was characterized by 22 groups of trials according to a 11 (10 active spots + 1 sham condition) x 2 (conditions of interest: left vs. right-hand responses; or left vs. right visual stimuli; or hand vs. foot responses); C) Removal of outliers (+/- 2 Standard Deviations) from each of the trial groups; D) Comparison between active spot trials and sham trials within experimental condition of interest by means of t-statistics. In this way each participant was characterized by 20 single t-values according to a 2 (factors of interest) x 10 (active TMS spots). Such single t-values expressed the individual effect of TMS compared to sham stimulation at each of the TMS active sites and were the experimental data of interest for the following principal analysis performed at the group level.

Main group analysis: E) In a first-level analysis we first considered each of the 2 t-maps separately (i.e. those showing the effect of TMS compared to sham stimulation in each of the 2 factors of interest – 2 left columns of Figure 3). The data from each of the 10 active spots was compared to the null hypothesis of [mean value = 0]. This produced a map of 10 t-values accounting for the entire population of subjects. We tested 16 subjects using 10 multiple comparisons, therefore significance threshold was calculated on 15 degrees of freedom and corrected by 10 multiple comparisons. This corresponded to a t-value of 3.29 and a p-value of 0.005. Any TMS spot on the map showing a t-value outside the threshold levels (-3.29 - +3.29) indicated a significant effect of TMS compared to sham stimulation on RTs in that particular experimental condition. Since t-values have a polarity, negative t-values indicate shortened RTs, and positive t-values indicate increased RTs in the active TMS compared to sham. F) In a second-level analysis we compared, for each TMS site the t-values in one condition (in the current example, right-hand responses) with the t-values in the other condition (in the current example, left-hand responses), by means of a paired-sample t-test. The resulting map of 10 t-values (one for

each TMS spot) indicated where on the grid active TMS had different effects between the two experimental conditions and represented the main output of the experiment (Figure 3). Note that this means that lack of a reliable effect at this level of analysis implies no statistical difference between the two conditions of interest, but this is still compatible with the possibility that TMS had a strong effect relative to the sham, an equal effect between the two conditions of interest. Additionally, the 10-point map was smoothed to obtain a surface plot, as follows:

Rendering and illustration: G) The data from the 2-dimensional spatial map defined by the 10 TMS spots were interpolated by means of the MATLAB 'meshgrid' command. In the resulting map of t-values, the data were highlighted according to the critical t-level for significance (+3.29 or -3.29). The resulting final contour map, represented in the illustrations to the present work, indicates the regions where the t-value is beyond the significance threshold.

Planned comparisons of interest: The whole data processing procedure was repeated for every comparison of interest. The paired comparisons were planned a priori according to the experimental hypotheses. We performed the following comparisons according to the main experimental hypotheses: 1) Foot responses vs. hand responses. 2) Left hand responses vs. right hand responses. 3) Hand responses to left stimuli vs. hand responses to right stimuli. 4) Left foot responses vs. right foot responses. 5) Foot responses to left stimuli vs. foot responses to right stimuli. In addition, we explored the issue of stimulus-response compatibility, limitedly to hand movements. We plotted the t-maps of congruent conditions: 1) Left hand responses to left stimuli and 2) Right hand responses to right stimuli, and of incongruent conditions: 3) Left hand responses to right stimuli and 4) Right hand responses to left stimuli.

Analysis on stimulus-response compatibility effects. We tested the presence of a behavioral stimulus-response compatibility (S-RC, Simon effect) effect in hand-responses by re-grouping the trials according to the congruence between the response stimulus and the response side, thus

categorizing the data as compatible versus incompatible trials only on hand movements. We submitted these RT values to an ANOVA with SRC (compatible vs. incompatible) as a within-subjects variable. According to the literature, an increase in RTs is expected as the behavioral marker of the “cost of incongruency” between stimulus and response. At a second stage we explored the possibility that TMS over a single spot of the cortical grid might influence the S-RC effect, measured as the difference in performance between S-R incompatible trials and S-R compatible trials. To do so we could not adopt the same mapping procedure as described above, because the current analysis is performed on a differential index (the S-R compatibility index) that can only be computed between average values of RTs. The main analysis, based on single trial values, could not be adopted. For each participant, we first processed the RTs by removing outliers (as described in the main analysis) and then we calculated the difference between mean RTs in incompatible trials minus the mean RTs in compatible trials. We then performed a paired-data t-test at population level between the S-RC indexes in the sham condition and those in each of the 10 spots. This analysis was carried out on the whole dataset and also on two subsets in which responses had been given with the left or the right effector. The significance threshold was therefore corrected for 30 multiple comparisons to p=0.00017.

RESULTS

None of the participants reported significant immediate or delayed side effects. The procedure was generally well-tolerated despite the considerable duration of the experiment, owing to the frequent breaks and the partitioning in two experimental sessions. The results of the experiment are illustrated in Figure 3. The statistical parameters for each point are shown in Table 1. Mean RT and standard deviation in ms for each point and for each condition of interest are shown in Table 2. In all conditions, the effects of TMS compared to sham stimulation were represented by a decrease in RTs, i.e. an improvement in performance. The whole dataset and the scripts used for data analysis are available online at 'https://osf.io/t6cp9/', stored on the Open Science Framework data sharing platform (Foster and Deardorff 2017). A descriptive account of the topography of the results in all conditions of interest is detailed hereafter:

Hand vs. Foot actions: TMS shortened RTs compared to sham stimulation when applied to a large premotor region (points 3, 5, 6, 7, 9), encompassing the dorsal and the ventral sectors, in the case of hand movements (Fig. 3A) and a smaller region (points 2, 4, 5) located more dorsally and posteriorly for foot actions (Fig. 3B), apparently limited to the dorsal premotor cortex. There was partial overlap between the hand- and foot-representations, but one point (6) showed a significant difference between the two (Fig. 3, A > B).

Right Hand vs. Left Hand actions: TMS shortened significantly the reaction times of right-hand responses when applied to a region in the mid-dorsal premotor cortex (spots 3, 5, 6, 8) (Fig. 3C). Left-hand responses were affected by TMS applied to two distant foci, an anterior dorsal region (6) and a ventral region (7, 9) (Fig. 3D), non-overlapping with the area representing the contralateral movements. Direct comparison between right and left-hand movements showed a significant differential effect of TMS in the ventral premotor cortex (9) (Fig. 3, C > D).

Right Foot vs. Left Foot actions: TMS affected performance when applied to a dorsal spot (2) for right foot responses and to a dorsal-posterior spot (spot 4) for left-foot responses (Fig. 3G and 3H). Despite the non-overlap of the two spots, the direct comparison between right and left foot actions did not show significant results.

Right-sided stimuli vs. Left-sided stimuli in hand actions: TMS affected performance in response to stimuli presented in the right hemispace (regardless of which hand was used to respond) when applied to a large region of the dorsal premotor cortex (2, 5, 6, 7) (Fig. 3E). Conversely, TMS affected hand responses to ipsilateral (left) stimuli when applied to an anterior dorsal premotor region (6) and to a ventral premotor spot (9) (Fig. 3F).

Right-sided stimuli vs. Left-sided stimuli in foot actions: TMS showed significant effects, compared to sham, only in responses to left-sided stimuli, when applied to a dorsal spot (4) (Fig. 3I and 3J).

Stimulus-response spatial congruency: We assessed the presence of a Simon effect separately for hand and foot actions, for both RTs and accuracy data. As expected, RTs analysis showed a significant effect of congruency for both hand ($F(1,15) = 55.05$, $p < .001$) and foot actions ($F(1,15) = 31.22$, $p < .001$), implying that participants were faster when response side and stimulus side were the same compared to different. Likewise, accuracy analysis revealed a significant main effect of congruency for both hand ($F(1,15) = 9.76$, $p = .006$) and foot actions ($F(1,15) = 1.04$, $p = .005$), indicating higher accuracy for the congruent compared to the incongruent condition (see Figure 4A).

Additional analyses: As additional analysis, for RTs only, we checked for potential "order effect" in the task, by computing an ANOVA with congruency (congruent vs. incongruent), stimulation site (11 grid hotspots) and session (first vs. second) as within-subject variables. Indeed, the analysis revealed a significant main effect of session, both for hand ($F(1,15) = 7.54$, $p = .014$)

and foot ($F(1,15) = 16.56$, $p = .001$) actions, reflecting faster RT in the second session, compared to the first session (hand: session 1, M= 323 ms, SD=55 ms; session 2, M= 305 ms, SD=61 ms; foot: session 1, M= 411 ms, SD=74 ms; session 2, M= 384 ms, SD=87 ms). Crucially, the factor session did not significantly interact with any of the other variables, all *p's* > .09. Finally, planned-comparisons t-tests were performed to assess whether the Simon effect was modulated by premotor stimulated points compared to the sham conditions. This analysis on single spots did not show any significant effect of TMS over sham on the cost of SRC in either the upper (minimum p-value=0.96) or the lower (minimum p-value=0.97) limb data (see Figure 4B). The same analysis was performed on accuracy data. Again, TMS did not significantly modulate the Simon effect for either the upper (minimum p-value=0.09) or the lower (minimum p-value=0.09) limb data (see Figure 4B).

DISCUSSION

Spatially-contingent behavior, such as reaching movements, are the basis of our interaction with the external world. They require the coexistence of a sensory mapping of personal and extra-personal space in extrinsic coordinates (the location of the selected target) and a motor representation of the effector selected for action. Here, we used d-TMS to map the role of the entire PM in producing spatially-dependent behavior in healthy human volunteers. Three key findings emerged: First, TMS affected hand-responses when applied to sites that were slightly anterior to those where foot-responses were affected, within the dorsal premotor cortex (foot actions were not affected by ventral premotor stimulations) as shown in Figure 3-upper row. Second, focusing on hand responses, contralateral (right) responses (Figure 3C) and responses to contralateral (right) targets (Figure 3E) were affected by TMS applied over a spot located in the mid-anterior portion of the dorsal PM. Third, ipsilateral responses (Figure 3D) and responses to ipsilateral targets (Figure 3F) seemed to be represented in a more widespread network comprising the dorsal and the ventral PM.

Effector-specific organization of the premotor cortex. The first observation demonstrated that foot actions are represented more dorsally and caudally compared to hand actions. Two effectors are not sufficient to define somatotopy, but we can safely conclude that hand and foot actions are spatially separate, though partially overlapping, in the dPM. The current results compare favorably with the few available data on somatotopy in the human dPM during voluntary movement. Indeed, congruently with our data, previous studies observed that activation for hand movement was typically located anterior to that observed for foot movement (Fink et al. 1997; Kollias et al. 2001). Additionally, our results also showed a larger cortical region implicated in hand actions compared to foot actions. Accordingly, less activation for foot movement compared to hand movement was reported in previous neuroimaging studies (Fink et al. 1997; Kollias et al.

2001). In a more recent study, a different distribution of effector-specific activity was found (Heed et al. 2016) along a medio-lateral axis rather than on the caudo-rostral axis. Starting at the precentral sulcus and extending forward to the PM, a stronger activation for hand on the lateral surface and for foot on the medial surface of the left hemisphere was shown (Heed et al. 2016). Functional imaging of covert motor activity such as in the processes of action observation or motor imagery provides similar evidence for a somatotopic organization of the PM (Buccino et al. 2001; Stippich et al. 2002; Ehrsson 2003; Wheaton et al. 2004; Sakreida 2005; Jastorff et al. 2010; Lorey et al. 2014). The present findings provide unique causal information on the spatial segregation of the PM regions necessary for the execution of action. The results are well-supported by previous indirect evidence from functional imaging.

Representation of effector side in the human premotor cortex. We found that the left PM contains a bilateral representation of the upper and lower limbs. This is unsurprising, in the context of previous functional imaging data (Medendorp et al. 2005; Beurze et al. 2007, 2009; Gallivan, McLean, Smith, et al. 2011; Gallivan et al. 2013). The task that we employed is a form of spatially-dependent behavior relying on a newly acquired abstract rule and according to previous monkey and human literature we expected such behavior to be supported by the dPM (Petrides 1985; Passingham 1989; Wise et al. 1996; Toni et al. 2001; Calton et al. 2002; Eliassen et al. 2003; Boettiger 2005; Medendorp et al. 2005; Hoshi and Tanji 2006, 2007, Beurze et al. 2007, 2009). Conversely, an unexpected result was the topographic localization of the ipsilateral and contralateral actions. Indeed, we found the topography of contralateral representation of action to be fully contained in the dPM, being all dorsal to the hotspot for the hand-primary motor cortex (see Figure 3). These findings confirm neuroimaging data, demonstrating a clear contralateral effector specificity localized in the dPM, but not in vPM (Beurze et al. 2007, 2009; Connolly et al. 2007) during visuo-motor integration for reaching movement.

The topography of ipsilateral action representation was, on the contrary, unexpected. We found only a partial overlap with the representation of contralateral actions, in the dPM, where TMS effects on ipsilateral actions were localized more rostrally. Interestingly, also a more ventral portion of PM was found to influence ipsilateral movements. Summing up, we found two clearly distinct cortical networks associated with motor behavior served by the contralateral and ipsilateral hand. With the current data we can only speculate on the actual functional level at which the vPM controls ipsilateral movements and not contralateral ones. The fact that we found only ipsilateral movements to be represented in vPM suggests that vPM's function might go beyond that of a sensorimotor association, but that it controls for surround, corollary activity, such as inhibition of the contralateral limbs (Buch et al. 2010). Furthermore, as a general point we would like to note that the findings here are not to be interpreted exclusively, as absence of evidence is not evidence of absence: When we say that a particular spot influenced significantly only ipsilateral representations, it does not mean that it contained solely ipsilateral representations. When we consider the single spots, the present data are not necessary in contradiction with previous findings. For example, Davare and colleagues (2006) found that TMS over the left and right PMv impaired the grasping component of movements performed with the right hand, which reinforces the present results, revealing that human PM contains both ipsilateral and contralateral hand representations. The real novelty of our data was to have compared multiple spots covering the whole left PM in a within-subjects design, thus unveiling a non-overlapping cortical region for ipsilateral and contralateral sensori-motor representations. Overall the literature tells us that the ventral precentral region is extremely complex. As such, within 1 cm of cortex researchers have localized: executive functions and conflict resolution (Brass et al. 2005), language (see Friederici 2006; Saur et al. 2008), action recognition (Gallese et al. 1996; Rizzolatti et al. 1996, 2002; Keysers et al. 2003; Binkofski and Buccino 2006) and action execution (Rizzolatti et

al. 2002, 2014; Binkofski and Buccino 2006; Filimon et al. 2007; Bonini et al. 2010, 2014). It remains to be understood whether the current effects on ipsilateral movements are due to the modulation of one or multiple of the cited functions. We interpret the dissonance of our data with the previous neuroimaging literature in several ways. First of all, focal TMS used as a behavior-changing tool yields more conservative results compared to functional neuroimaging. Areas that show functional activation for given tasks may actually fail to be associated with behavioral effects when stimulated. On a related topic, the TMS approach highlights exclusively the cortical regions that are causally related to the behavior of interest. Besides the different adopted method (TMS vs. neuroimaging vs. neurophysiological studies), it is also important to consider some crucial differences concerning the adopted paradigms between the present study and previous findings. Indeed, most studies in human and non-human primates focused on spatially-oriented behaviors predominantly adopting reaching/grasping tasks. As a cautionary note, the Simon task may indeed engage different sensorimotor computations compared to a reaching movement. In this light, the unexpected topography of ipsilateral action representation compared to previous investigations (Rizzolatti et al. 1988; Fogassi et al. 2001; Davare et al. 2006) might be at least partly dependent on the selected task. In this context, it remains to be seen whether and to what extent the present findings may be generalizable to other and more complex forms of sensori-motor associations, and that seems like a worthwhile subject of future dense TMS mapping investigation.

Representation of the stimulus side in the human premotor cortex. TMS applied to the left mid-anterior portion of the PM affected responses to contralateral (right) targets, despite spatial localization was task-irrelevant (participants had to respond to target's color). Crucially, the same spots also affected responses given with contralateral (right) effectors. Conversely, targets and responses ipsilateral to the stimulation were represented in a more widespread network comprising also the vPM. The neural representation of space in human premotor cortex is more

controversial compared to non-human primates: Our results suggest that a core region with the classical properties of monkeys' PMv (contralateral responses and contralateral stimuli) is localized more dorsally in human PM. However, it is important to note that several recent studies in non-human primates indicate that grasping-related neurons are not localized strictly in the ventral premotor cortex. Instead, these findings indicated that a wider premotor region at the boundary between the most dorsal part of the ventral premotor cortex and the adjacent ventro-rostral portion of the dorsal premotor cortex are regions densely populated by hand-related neurons (Raos et al. 2004; Bonini et al. 2014; Vargas-Irwin et al. 2015). Congruently, in a recent study, Papadourakis and Roas (Papadourakis and Raos 2018) demonstrated that neuronal responses between execution and observation, as well as the encoding of grip type are alike in both PMd and PMv, providing direct evidence of similarity between hand-related visual and motor representations in the macaque dPM. In line with these findings, the present study seems to suggest that the neural representation of sensorimotor processes may actually be very similar between the two-primate species. The present findings extend neuroimaging studies, demonstrating a direct role of the anterior portion of the human dPM in spatial coding. Accordingly, previous evidence from multivariate fMRI techniques showed a selective dPM involvement in target coding representation (Gallivan, McLean, Smith, et al. 2011; Fabbri et al. 2012; Cappadocia et al. 2017) as well as contralateral spatial selectivity during object-directed behavior (Beurze et al. 2007, 2009; Bernier et al. 2012; Chen et al. 2014). Furthermore, a critical role of dPM in sensory processing has been already demonstrated in previous studies showing a dPM engagement in spatial processing both in humans (Griffiths et al. 2000; Nobre et al. 2000; Lamm et al. 2001; Pochon 2001; Handy et al. 2003) and in non-human primates (Kubota and Hamada 1978; Passingham 1987; Boussaoud and Wise 1993; Shen and Alexander 1997; Lebedev and Wise 2001). Similarly, involvement of dPM in spatial transformation has been reported in

humans, whose activation seems to depend on the complexity of the spatial response structure (spatial transformations) of visually guided sequences (Harrington et al. 2000; Boecker 2002; Haslinger et al. 2002).

Congruent and incongruent sensorimotor associations. The Simon task is employed in experimental psychology to explore stimulus-response compatibility, i.e. the dimensional overlap (in this case spatial) between stimulus and response (Simon and Rudell 1967). Same-side stimuli and responses are "congruent" (or compatible) conditions and opposite-side stimulus-response associations are defined as "incongruent" (or incompatible). Incongruent conditions bear a cost in performance, indicated by slower response times (see Lu and Proctor 1995). In the present experiment we showed the expected behavioral pattern of congruent vs. incongruent trials. We mapped the effects of TMS vs. sham for left- or right-hand responses to left or right stimuli. The results showed that the single left premotor cortex contains neither a representation of S-R congruency *per se* nor dependently from the side of the stimuli or responses. Indeed, the right hand-right stimulus condition and the left-hand left stimulus condition, both belonging to the "congruent" category, showed a completely different cartography. We hypothesize that a specular pattern could be found in the right hemisphere and that the "congruence" is not a unique category represented somewhere in the brain, but it is strictly lateralized. It would be interesting for future investigation to explore this issue. The negative results we found for the left PM stimulation in mediating congruent and incongruent associations may appear at odds with previous studies both in human (Iacoboni et al. 1998; Praamstra et al. 1999; Bischoff-Grethe et al. 2004; Bardi et al. 2015) and non-human primates (Petrides 1985; Passingham 1993; Wise et al. 1996), convergently indicating a role of dPM in learning abstract, non-standard stimulus-response mapping and in resolving response conflict (Niendam et al. 2012 see). We hypothesized that our time-locked, dual pulses TMS stimulation 50 ms after the stimulus onset may have been

suboptimal for inducing clear-cut behavioral changes in respect to the congruent vs. incongruent effects. In line with this interpretation, Bardi and colleagues (2015) indeed reported an effect of left dPM TMS stimulation on the Simon effect. Notably, the authors found a selective decrease of the Simon effect when TMS was applied at 160 ms after stimulus onset and an increase of the Simon effect at later times (220-250 ms). Therefore, we cannot exclude the possibility that the early stimulation (between 50 and 150 ms after display onset) applied in the current study was not adequate for affecting the spatial-response conflict, and that a later or more prolonged stimulation (Praamstra et al. 1999) may reveal the involvement of left PM in the current behavioral context.

Facilitatory effects of TMS. It is important to notice that all TMS effects emerged in our study were exclusively facilitatory. The present findings receive support from previous studies that examined response selection and motor reprogramming and showed that the facilitatory versus inhibitory effect of dPM stimulation over M1 depended on the timing of the stimulation (Koch, Franca, Fernandez Del Olmo, et al. 2006; O'Shea et al. 2007; Buch et al. 2010). Two paired-pulse TMS studies investigated physiological and timing interaction between dPM and M1 during the execution of sensori-motor tasks. In both studies, results showed that dPM stimulation applied early after the stimulus onset (around 75 ms) facilitates M1 activity, whereas later stimulation delayed reaction times and suppressed the prepared movement (Koch, Franca, Fernandez Del Olmo, et al. 2006; O'Shea et al. 2007).

The design of our experiment does not allow us to draw final conclusions about hemispheric asymmetries. By unveiling a selective TMS effect for both contralateral stimuli and responses, the present results do not seem to support the left hemisphere dominance in response selection reported in previous studies (Schluter et al. 1998, 2001; Johansen-Berg et al. 2002; Mochizuki et al. 2005; Bardi et al. 2015). However, it is noteworthy that the inter-manual

differences with respect to interhemispheric interaction between dPM and M1 remain today an open question, with inconsistent results (Koch, Franca, Fernandez Del Olmo, et al. 2006; O'Shea et al. 2007). For instance, O'Shea and colleagues (O'Shea et al. 2007) studied the functional connection between dPM and primary motor cortex (M1) by means of paired-pulse TMS and reported comparable effects of conditioning TMS of left and right dPM, suggesting no hemispheric asymmetries in dPM-M1 interaction during response selection. Although this was not the focus of the present study, the present findings showed that TMS over the left dPM selectively affected motor and sensory contralateral representations. However, this point deserves further consideration. For instance, it would be interesting for future investigations to specifically compare TMS effects while mapping both the left and right PM in object-directed behaviors. The execution of spatially-oriented motor behaviors requires complex interactions between premotor and primary motor areas in the two hemispheres. The causal interaction between different sectors of the premotor cortex and primary motor cortices are still scarcely known. In particular, where and how those interactions are supported by direct corticospinal projections, or by indirect cortico-cortical pathways is still poorly understood. Interestingly, in line with the present findings, previous dual coil TMS studies testing long-latency interactions between premotor and motor cortices, demonstrated different modulatory effects of ventral, dorsal and supplementary premotor stimulation on corticospinal output (Mochizuki et al. 2004; Ni et al. 2009; Fiori et al. 2016, 2017, 2018).

TMS statistical mapping. Finally, the present study supports the use of TMS as an effective brain mapping tool. The use of TMS statistical mapping has been successfully used in previous studies (Stoeckel et al. 2009; Cattaneo and Barchiesi 2011; Maule et al. 2015; Fricke et al. 2017): This method gives more detailed information compared to TMS studies adopting the *a priori* localization of coil positioning (Cattaneo 2018). Such approach appears to be a promising tool for

mapping defined brain regions of interest. This consideration is especially valid for non-uniform regions, comprising several subdivisions with specialized function and connectivity, such as the PM (Genon et al. 2016). However, the use of TMS for brain mapping in dense arrays, as any other spatial sampling procedure requires that the sampling is evenly distributed and that the spatial sampling frequency is adequate to avoid aliasing in the reconstruction of a sampled signal (see Cattaneo (2018) for a discussion on this topic). According to the Shannon-Nyquist theorem, sampling rate should be at least twice the maximum frequency of the signal to be sampled (Shannon 1949). In the present experiment the cortical space has been sampled every 2 cm on the scalp, which corresponds to around 1.6 cm on the cortical surface (approximating the scalp and brain as concentric spheres with radial distance between them of 1.5 cm). This said, the spatial sampling frequency adopted here is adequate for sampling topographic signals that change roughly every 3 cm. This compares favorably with current functional parcellation maps of the human premotor cortex (Buccino et al. 2001; Tomassini et al. 2007; Schubotz et al. 2010; Sallet et al. 2013; Genon et al. 2016, 2018), but it should be kept in mind that the present spatial sampling procedure would fail to detect features with finer granularity.

Limitations of the study. The empirical results reported herein should be considered in the light of some limitations. First, the design of our experiment does not allow to draw firm conclusions concerning the functional role of the entire premotor cortex in spatially-dependent sensorimotor functions. While the present findings strongly contribute to the debate about the selective functional role of each sub-region of the premotor cortex, a more comprehensive discussion about laterality would also require the stimulation of the right hemisphere. Human literature shows a left-right asymmetry in the premotor regions, with left premotor cortex influencing behaviour that is performed unilaterally with either side of the brain and right premotor cortex influencing only left movements (Schluter et al. 1998, 2001; Johansen-Berg et al.

2002; Koch, Franca, Del Olmo, et al. 2006; O'Shea et al. 2007; Bardi et al. 2015). Our expectation would therefore be that the contralateral representations of movement and stimuli is probably symmetrical. Conversely, some asymmetry could be found on the ipsilateral representations. This step is necessary to draw an exhaustive functional cartography of the premotor cortex in sensorimotor processes and represents a natural extension of the present study to further explore in future investigations. Other limitations concern methodological aspects. Indeed, in the present study the inter-trial interval was kept constant at 4000 ms throughout the experiment. This may be not the best option, since it introduces a strong effect of expectancy. Future investigations may consider adopting a temporal jitter to avoid effects linked to subjects' expectancy. Another issue regards the neuronavigation procedure. Previous TMS studies functionally localized both PMd and PMv starting from the individual M1 (Bäumer et al. 2009; Ortu et al. 2009; Bardi et al. 2015; Lega et al. 2016). In the present study, the grid over premotor regions was determined with reference to the individual hand, foot and mouth M1, which allowed us to consistently localize in each subject the medial, dorsal and ventral sectors of PM. Nonetheless, the use of individual MRI together with a neuronavigation system might have been a more suitable choice in order to be sure that the very same targets were used in all subjects. This aspect should be borne in mind in the interpretation of the current results and it would be interesting for future studies to compare the present results by adopting a different TMS localization approach. A further potential source of bias is the use of the same intensity of stimulation (a function of the hand resting motor threshold) over all the spots of the premotor grid. In general, using individual RMT to dose individual TMS intensity on non-motor areas is aimed at reducing the inter-individual variability due to variable scalp-brain distance. Given that scalp-brain distance varies throughout the brain, it is possible to adjust stimulation intensity according to MRI-measured scalp-brain distance (Stokes et al. 2007). In our case most of the spots were in a region of uniform scalp-brain distance, similar

to that in the hand-related motor cortex (Okamoto et al. 2004), with the exception of the 3 more medial spots, in which the cortex dives deep into the inter-hemispheric fissure. Stimulation of the medial walls at high intensities, however, necessarily engages stimulation of the whole of the convexity near the lip of the inter-hemispheric fissure because higher intensities produce magnetic fields of larger volumes, compromising the rationale of the work, i.e. to perform a dense and even sampling of the cortex. We assumed therefore that the lesser experimental bias would have been achieved using the same stimulation intensities on all spots, knowing that the stimulation over the medial regions could reach only the dorsal half of the SMA and not all of it.

In conclusion, using a dense TMS spatial mapping approach, the present findings consistently demonstrated that the contralateral features (stimuli or actions) are represented in a mid-dorsal premotor core region. Instead, ipsilateral behavior is represented in the PM in a spatially non-overlapping network, that includes a more anterior dorsal premotor region and the ventral premotor cortex. Taken together, we suggest that contralateral and ipsilateral features are supported by two distinct and only partially overlapping cortical networks.

Acknowledgements: This work was supported by the Fondo Unico per la Ricerca (FUR) of the University of Verona.

References

Aizawa H, Mushiake H, Inase M, Tanji J. 1990. An output zone of the monkey primary motor cortex specialized for bilateral hand movement. Exp Brain Res. 82.

Amunts K, Schleicher A, Zilles K. 2007. Cytoarchitecture of the cerebral cortex - more than localization. Neuroimage 37: 1061-1065

Bardi L, Schiff S, Basso D, Mapelli D. 2015. A transcranial magnetic stimulation study on response activation and selection in spatial conflict. Eur J Neurosci. 41:487–491.

Baumann MA, Fluet M-C, Scherberger H. 2009. Context-Specific Grasp Movement Representation in the Macaque Anterior Intraparietal Area. J Neurosci. 29:6436–6448.

Bäumer T, Schippling S, Kroeger J, Zittel S, Koch G, Thomalla G, Rothwell JC, Siebner HR, Orth M, Münchau A. 2009. Clinical Neurophysiology Inhibitory and facilitatory connectivity from ventral premotor to primary motor cortex in healthy humans at rest – A bifocal TMS study. Clin Neurophysiol. 120:1724–1731.

Bernier PM, Cieslak M, Grafton ST. 2012. Effector selection precedes reach planning in the dorsal parietofrontal cortex. J Neurophysiol. 108:57–68.

Beurze SM, de Lange FP, Toni I, Medendorp WP. 2007. Integration of Target and Effector Information in the Human Brain During Reach Planning. J Neurophysiol. 97:188–199.

Beurze SM, de Lange FP, Toni I, Medendorp WP. 2009. Spatial and Effector Processing in the Human Parietofrontal Network for Reaches and Saccades. J Neurophysiol. 101:3053–3062.

Binkofski F, Buccino G. 2006. The role of ventral premotor cortex in action execution and action understanding. J Physiol. 99:396–405.

Bischoff-Grethe A, Goedert KM, Willingham DT, Grafton ST. 2004. Neural Substrates of Response-based Sequence Learning using fMRI. J Cogn Neurosci. 16:127–138.

Boecker H. 2002. A H215O Positron Emission Tomography Study on Mental Imagery of Movement Sequences—The Effect of Modulating Sequence Length and Direction. Neuroimage. 17:999–1009.

Boettiger CA. 2005. Frontal Networks for Learning and Executing Arbitrary Stimulus-Response Associations. J Neurosci. 25:2723–2732.

Bonini L. 2017. The Extended Mirror Neuron Network: Anatomy, Origin, and Functions. Neuroscientist.

Bonini L, Maranesi M, Livi A, Fogassi L, Rizzolatti G. 2014. Ventral premotor neurons encoding representations of action during self and others' inaction. Curr Biol. 24:1611–1614.

Bonini L, Rozzi S, Serventi FU, Simone L, Ferrari PF, Fogassi L. 2010. Ventral Premotor and Inferior Parietal Cortices Make Distinct Contribution to Action Organization and Intention Understanding. Cereb Cortex. 20:1372–1385.

Bonini L, Ugolotti Serventi F, Bruni S, Maranesi M, Bimbi M, Simone L, Rozzi S, Ferrari PF, Fogassi L. 2012. Selectivity for grip type and action goal in macaque inferior parietal and ventral premotor grasping neurons. J Neurophysiol. 108:1607–1619.

Borra E, Gerbella M, Rozzi S, Luppino G. 2017. The macaque lateral grasping network: A neural

substrate for generating purposeful hand actions. Neurosci Biobehav Rev. 75:65–90.

Boussaoud D, Wise SP. 1993. Primate frontal cortex: neuronal activity following attentional versus intentional cues. Exp Brain Res. 95:15–27.

Brass M, Derrfuss J, Forstmann B, Von Cramon DY. 2005. The role of the inferior frontal junction area in cognitive control. Trends Cogn Sci.

Brochier T, Umiltà MA. 2007. Cortical control of grasp in non-human primates. Curr Opin Neurobiol. 17:637–643.

Buccino G, Binkofski F, Fink GR, Fadiga L, Fogassi L, Gallese V, Seitz RJ, Zilles K, Rizzolatti G, Parma Á, Volturno V, Parma I-. 2001. Action observation activates premotor and parietal areas in a somatotopic manner an fMRI. 13:400–404.

Buch ER, Mars RB, Boorman ED, Rushworth MFS. 2010. A Network Centered on Ventral Premotor Cortex Exerts Both Facilitatory and Inhibitory Control over Primary Motor Cortex during Action Reprogramming. J Neurosci. 30:1395–1401.

Busan P, Barbera C, Semenic M, Monti F, Pizzolato G, Pelamatti G, Battaglini PP. 2009. Effect of Transcranial Magnetic Stimulation (TMS) on Parietal and Premotor Cortex during Planning of Reaching Movements. PLoS One. 4:e4621.

Calton JL, Dickinson AR, Snyder LH. 2002. Non-spatial, motor-specific activation in posterior parietal cortex. Nat Neurosci. 5:580–588.

Caminiti R, Innocenti GM, Battaglia-Mayer A. 2015. Organization and evolution of parieto-frontal processing streams in macaque monkeys and humans. Neurosci Biobehav Rev. 56:73–96.

Caminiti R, Johnson P, Galli C, Ferraina S, Burnod Y. 1991. Making arm movements within different parts of space: the premotor and motor cortical representation of a coordinate system for reaching to visual targets. J Neurosci. 11:1182–1197.

Cappadocia DC, Monaco S, Chen Y, Blohm G, Crawford JD. 2017. Temporal Evolution of Target Representation, Movement Direction Planning, and Reach Execution in Occipital-Parietal-Frontal Cortex: An fMRI Study. Cereb Cortex. 27:5242–5260.

Cattaneo L. 2018. Fancies and Fallacies of Spatial Sampling With Transcranial Magnetic Stimulation (TMS). Front Psychol. 9.

Cattaneo L, Barchiesi G. 2011. Transcranial Magnetic Mapping of the Short-Latency Modulations of Corticospinal Activity from the Ipsilateral Hemisphere during Rest. Front Neural Circuits. 5:1–13.

Chen Y, Monaco S, Byrne P, Yan X, Henriques DYP, Crawford JD. 2014. Allocentric versus Egocentric Representation of Remembered Reach Targets in Human Cortex. J Neurosci. 34:12515–12526.

Cisek P, Crammond DJ, Kalaska JF. 2003. Neural Activity in Primary Motor and Dorsal Premotor Cortex In Reaching Tasks With the Contralateral Versus Ipsilateral Arm. J Neurophysiol. 89:922–942.

Cisek P, Kalaska JF. 2010. Neural Mechanisms for Interacting with a World Full of Action Choices. Annu Rev Neurosci. 33:269–298.

Connolly JD, Goodale MA, Cant JS, Munoz DP. 2007. Effector-specific fields for motor preparation in the human frontal cortex. Neuroimage. 34:1209–1219.

Davare M, Andres M, Cosnard G, Thonnard J-L, Olivier E. 2006. Dissociating the role of ventral and dorsal premotor cortex in precision grasping. J Neurosci. 26:2260–2268.

Donchin O, Gribova A, Steinberg O, Bergman H, Vaadia E. 1998. Primary motor cortex is involved in bimanual coordination. Nature. 395:274–278.

Ehrsson HH. 2003. Imagery of Voluntary Movement of Fingers, Toes, and Tongue Activates Corresponding Body-Part-Specific Motor Representations. J Neurophysiol. 90:3304–3316.

Eliassen JC, Souza T, Sanes JN. 2003. Experience-dependent activation patterns in human brain during visual-motor associative learning. J Neurosci. 23:10540–10547.

Fabbri S, Caramazza A, Lingnau A. 2012. Distributed sensitivity for movement amplitude in directionally tuned neuronal populations. J Neurophysiol. 107:1845–1856.

Fabbri S, Strnad L, Caramazza A, Lingnau A. 2014. Overlapping representations for grip type and reach direction. Neuroimage. 94:138–146.

Fattori P, Breveglieri R, Raos V, Bosco A, Galletti C. 2012. Vision for Action in the Macaque Medial Posterior Parietal Cortex. J Neurosci. 32:3221–3234.

Fattori P, Raos V, Breveglieri R, Bosco A, Marzocchi N, Galletti C. 2010. The Dorsomedial Pathway Is Not Just for Reaching: Grasping Neurons in the Medial Parieto-Occipital Cortex of the Macaque Monkey. J Neurosci. 30:342–349.

Filimon F, Nelson JD, Hagler DJ, Sereno MI. 2007. Human cortical representations for reaching: Mirror neurons for execution, observation, and imagery. Neuroimage. 37:1315–1328.

Fink GR, Frackowiak RSJ, Pietrzyk U, Passingham RE. 1997. Multiple nonprimary motor areas in the human cortex. J Neurophysiol. 77:2164–2174.

Fiori F, Chiappini E, Avenanti A. 2018. Enhanced action performance following TMS manipulation of associative plasticity in ventral premotor-motor pathway. Neuroimage. 183:847–858.

Fiori F, Chiappini E, Candidi M, Romei V, Borgomaneri S, Avenanti A. 2017. Long-latency interhemispheric interactions between motor-related areas and the primary motor cortex: a dual site TMS study. Sci Rep. 7:14936.

Fiori F, Chiappini E, Soriano M, Paracampo R, Romei V, Borgomaneri S, Avenanti A. 2016. Long-latency modulation of motor cortex excitability by ipsilateral posterior inferior frontal gyrus and pre-supplementary motor area. Sci Rep. 6:38396.

Fluet M-C, Baumann MA, Scherberger H. 2010. Context-Specific Grasp Movement Representation in Macaque Ventral Premotor Cortex. J Neurosci. 30:15175–15184.

Fogassi L, Gallese V, Buccino G, Craighero L, Fadiga L, Rizzolatti G. 2001. Cortical mechanism for the visual guidance of hand grasping movements in the monkey: A reversible inactivation study. Brain. 124:571–586.

Foster ED, Deardorff A. 2017. Open Science Framework (OSF). J Med Libr Assoc.

Fricke C, Gentner R, Rumpf JJ, Weise D, Saur D, Classen J. 2017. Differential spatial representation of precision and power grasps in the human motor system. Neuroimage. 158:58–69.

Friederici AD. 2006. Broca's area and the ventral premotor cortex in language: Functional differentiation and specificity. Cortex. 42:472–475.

Gallese V, Fadiga L, Fogassi L, Rizzolatti G. 1996. Action recognition in the premotor cortex. Brain.

119:593–609.

Gallivan JP, Culham JC. 2015. Neural coding within human brain areas involved in actions. Curr Opin Neurobiol. 33:141–149.

Gallivan JP, McLean DA, Flanagan JR, Culham JC. 2013. Where One Hand Meets the Other: Limb-Specific and Action-Dependent Movement Plans Decoded from Preparatory Signals in Single Human Frontoparietal Brain Areas. J Neurosci. 33:1991–2008.

Gallivan JP, McLean DA, Smith FW, Culham JC. 2011. Decoding Effector-Dependent and Effector-Independent Movement Intentions from Human Parieto-Frontal Brain Activity. J Neurosci. 31:17149–17168.

Gallivan JP, McLean DA, Valyear KF, Pettypiece CE, Culham JC. 2011. Decoding Action Intentions from Preparatory Brain Activity in Human Parieto-Frontal Networks. J Neurosci. 31:9599–9610.

Ganguly K, Secundo L, Ranade G, Orsborn A, Chang EF, Dimitrov DF, Wallis JD, Barbaro NM, Knight RT, Carmena JM. 2009. Cortical Representation of Ipsilateral Arm Movements in Monkey and Man. J Neurosci. 29:12948–12956.

Genon S, Li H, Fan L, Müller VI, Cieslik EC, Hoffstaedter F, Reid AT, Langner R, Grefkes C, Fox PT, Moebus S, Caspers S, Amunts K, Jiang T, Eickhoff SB. 2016. The Right Dorsal Premotor Mosaic: Organization, Functions, and Connectivity. Cereb Cortex. 27(3):2095–2110.

Genon S, Reid A, Li H, Fan L, Müller VI, Cieslik EC, Hoffstaedter F, Langner R, Grefkes C, Laird AR, Fox PT, Jiang T, Amunts K, Eickhoff SB. 2018. The heterogeneity of the left dorsal premotor cortex evidenced by multimodal connectivity-based parcellation and functional characterization. Neuroimage. 170:400–411.

Gentilucci M, Fogassi L, Luppino G, Matelli M, Camarda R, Rizzolatti G. 1988. Functional organization of inferior area 6 in the macaque monkey. Exp Brain Res. 71:475–490.

Gerbella M, Rozzi S, Rizzolatti G. 2017. The extended object-grasping network. Exp Brain Res. 235:2903–2916.

Geyer S, Matelli M, Luppino G, Zilles K. 2000. Functional neuroanatomy of the primate isocortical motor system. Anat Embryol (Berl). 202:443–474.

Gharbawie OA, Stepniewska I, Qi H, Kaas JH. 2011. Multiple Parietal-Frontal Pathways Mediate Grasping in Macaque Monkeys. J Neurosci. 31:11660–11677.

Graziano MSA. 2009. The Intelligent Movement Machine : an Ethological Perspective on the Primate Motor System. Oxford University Press.

Griffiths TD, Green GGR, Rees A, Rees G. 2000. Human brain areas involved in the analysis of auditory movement. Hum Brain Mapp. 9:72–80.

Handy TC, Grafton ST, Shroff NM, Ketay S, Gazzaniga MS. 2003. Graspable objects grab attention when the potential for action is recognized. Nat Neurosci. 6:421–427.

Harrington DL, Rao SM, Haaland KY, Bobholz JA, Mayer AR, Binder JR, Cox RW. 2000. Specialized Neural Systems Underlying Representations of Sequential Movements. J Cogn Neurosci. 12:56–77.

Hasbroucq T, Guiard Y. 1991. Stimulus-response compatibility and the Simon effect: Toward a conceptual clarification. J Exp Psychol Hum Percept Perform. 17:246–266.

Haslinger B, Erhard P, Weilke F, Ceballos-Baumann AO, Bartenstein P, Gräfin von Einsiedel H, Schwaiger M, Conrad B, Boecker H. 2002. The role of lateral premotor-cerebellar-parietal circuits in motor sequence control: A parametric fMRI study. Cogn Brain Res. 13:159–168.

Heed T, Leone FTM, Toni I, Medendorp WP. 2016. Functional versus effector-specific organization of the human posterior parietal cortex: revisited. J Neurophysiol. 116:1885–1899.

Hoshi E, Tanji J. 2006. Differential involvement of neurons in the dorsal and ventral premotor cortex during processing of visual signals for action planning. J Neurophysiol. 95:3596–3616.

Hoshi E, Tanji J. 2007. Distinctions between dorsal and ventral premotor areas: anatomical connectivity and functional properties. Curr Opin Neurobiol. 17:234–242.

Iacoboni M, Woods RP, Mazziotta JC. 1998. Bimodal (auditory and visual) left frontoparietal circuitry for sensorimotor integration and sensorimotor learning. Brain. 121:2135–2143.

Janssen P, Verhoef B-E, Premereur E. 2018. Functional interactions between the macaque dorsal and ventral visual pathways during three-dimensional object vision. Cortex. 98:218–227.

Jastorff J, Begliomini C, Fabbri-Destro M, Rizzolatti G, Orban GA. 2010. Coding Observed Motor Acts: Different Organizational Principles in the Parietal and Premotor Cortex of Humans. J Neurophysiol. 104:128–140.

Jeannerod M, Arbib MA, Rizzolatti G, Sakata H. 1995. Grasping objects: the cortical mechanisms of visuomotor transformation. Trends Neurosci. 18:314–320.

Johansen-Berg H, Rushworth MFS, Bogdanovic MD, Kischka U, Wimalaratna S, Matthews PM. 2002. The role of ipsilateral premotor cortex in hand movement after stroke. Proc Natl Acad Sci. 99:14518–14523.

Kermadi Y, Liu EM, Rouiller I. 2000. Do bimanual motor actions involve the dorsal premotor (PMd), cingulate (CMA) and posterior parietal (PPC) cortices? Comparison with primary and supplementary motor cortical areas. Somatosens Mot Res. 17:255–271.

Keysers C, Kohler E, Umiltà MA, Nanetti L, Fogassi L, Gallese V. 2003. Audiovisual mirror neurons and action recognition. In: Experimental Brain Research. p. 628–636.

Koch G, Franca M, Del Olmo MF, Cheeran B, Milton R, Alvarez Sauco M, Rothwell JC. 2006. Time course of functional connectivity between dorsal premotor and contralateral motor cortex during movement selection. J Neurosci. 26:7452–7459.

Koch G, Franca M, Fernandez Del Olmo M, Cheeran B, Milton R, Alvarez Sauco M, Rothwell JC. 2006. Time Course of Functional Connectivity between Dorsal Premotor and Contralateral Motor Cortex during Movement Selection. J Neurosci. 26:7452–7459.

Kollias SS, Alkadhi H, Jaermann T, Crelier G, Hepp-Reymond M-C. 2001. Identification of multiple nonprimary motor cortical areas with simple movements. Brain Res Rev. 36:185–195.

Kornblum S, Hasbroucq T, Osman A. 1990. Dimensional Overlap: Cognitive Basis for Stimulus-Response Compatibility-A Model and Taxonomy. Psychol Rev. 97:253–270.

Kubota K, Hamada I. 1978. Visual tracking and neuron activity in the post-arcuate area in monkeys. J Physiol (Paris). 74:297–312.

Lamm C, Windischberger C, Leodolter U, Moser E, Bauer H. 2001. Evidence for premotor cortex activity during dynamic visuospatial imagery from single-trial functional magnetic resonance imaging and event-related slow cortical potentials. Neuroimage. 14:268–283.

Lanzilotto M, Livi A, Maranesi M, Gerbella M, Barz F, Ruther P, Fogassi L, Rizzolatti G, Bonini L. 2016. Extending the cortical grasping network: Pre-supplementary motor neuron activity during vision and grasping of objects. Cereb Cortex. 26:4435–4449.

Lebedev MA, Wise SP. 2001. Tuning for the orientation of spatial attention in dorsal premotor cortex. Eur J Neurosci. 13:1002–1008.

Lebedev MA, Wise SP. 2002. Insights Into Seeing and Grasping: Distinguishing the Neural Correlates of Perception and Action. Behav Cogn Neurosci Rev. 1:108–129.

Lega C, Stephan MA, Zatorre RJ, Penhune V. 2016. Testing the role of dorsal premotor cortex in auditory-motor association learning using Transcranical Magnetic Stimulation (TMS). PLoS One.

Lehmann SJ, Scherberger H. 2013. Reach and Gaze Representations in Macaque Parietal and Premotor Grasp Areas. J Neurosci. 33:7038–7049.

Lehmann SJ, Scherberger H. 2015. Spatial Representations in Local Field Potential Activity of Primate Anterior Intraparietal Cortex (AIP). PLoS One. 10:e0142679.

Lisanby SH, Gutman D, Luber B, Schroeder C, Sackeim HA. 2001. Sham TMS: intracerebral measurement of the induced electrical field and the induction of motor-evoked potentials. Biol Psychiatry. 49:460–463.

Livi A, Lanzilotto M, Maranesi M, Fogassi L, Rizzolatti G, Bonini L. 2019. Agent-based representations of objects and actions in the monkey pre-supplementary motor area. Proc Natl Acad Sci. 116:2691–2700.

Lorey B, Naumann T, Pilgramm S, Petermann C, Bischoff M, Zentgraf K, Stark R, Vaitl D, Munzert J. 2014. Neural simulation of actions: Effector- versus action-specific motor maps within the human premotor and posterior parietal area? Hum Brain Mapp. 35:1212–1225.

Lu C, Proctor RW. 1995. The influence of irrelevant location information on performance: A review of the Simon and spatial Stroop effects. Psychon Bull Rev. 2:174–207.

Luppino G, Matelli M, Camarda RM, Gallese V, Rizzolatti G. 1991. Multiple representations of body movements in mesial area 6 and the adjacent cingulate cortex: An intracortical microstimulation study in the macaque monkey. J Comp Neurol. 311:463–482.

Mathôt S, Schreij D, Theeuwes J. 2012. OpenSesame: An open-source, graphical experiment builder for the social sciences. Behav Res Methods. 44:314–324.

Maule F, Barchiesi G, Brochier T, Cattaneo L. 2015. Haptic working memory for grasping: The role of the parietal operculum. Cereb Cortex. 25:528–537.

Medendorp WP, Goltz HC, Crawford JD, Vilis T. 2005. Integration of Target and Effector Information in Human Posterior Parietal Cortex for the Planning of Action. J Neurophysiol. 93:954–962.

Mitz AR, Wise SP. 1987. The somatotopic organization of the supplementary motor area: intracortical microstimulation mapping. J Neurosci. 7:1010–1021.

Mochizuki H, Franca M, Huang Y-Z, Rothwell JC. 2005. The role of dorsal premotor area in reaction task: comparing the “virtual lesion” effect of paired pulse or theta burst transcranial magnetic stimulation. Exp Brain Res. 167:414–421.

Mohlberg H, Eickhoff SB, Schleicher A, Zilles K, Amunts K. 2012. A new processing pipeline and

release of cytoarchitectonic probabilistic maps - JuBrain, OHBM 2012, Peking, China

Mochizuki H, Terao Y, Okabe S, Furubayashi T, Arai N, Iwata N, Hanajima R, Kamakura K, Motoyoshi K, Ugawa Y. 2004. Effects of motor cortical stimulation on the excitability of contralateral motor and sensory cortices. Exp Brain Res. 158.

Monaco S, Gallivan JP, Figley TD, Singhal A, Culham JC. 2017. Recruitment of Foveal Retinotopic Cortex During Haptic Exploration of Shapes and Actions in the Dark. J Neurosci. 37:11572–11591.

Monaco S, Sedda A, Cavina-Pratesi C, Culham JC. 2015. Neural correlates of object size and object location during grasping actions. Eur J Neurosci. 41:454–465.

Murata A, Fadiga L, Fogassi L, Gallese V, Raos V, Rizzolatti G. 1997. Object representation in the ventral premotor cortex (area F5) of the monkey. J Neurophysiol. 78:2226–2230.

Ni Z, Gunraj C, Nelson AJ, Yeh I-J, Castillo G, Hoque T, Chen R. 2009. Two Phases of Interhemispheric Inhibition between Motor Related Cortical Areas and the Primary Motor Cortex in Human. Cereb Cortex. 19:1654–1665.

Niendam TA, Laird AR, Ray KL, Dean YM, Glahn DC, Carter CS. 2012. Meta-analytic evidence for a superordinate cognitive control network subserving diverse executive functions. Cogn Affect Behav Neurosci. 12:241–268.

Nobre AC, Gitelman DR, Dias EC, Mesulam MM. 2000. Covert Visual Spatial Orienting and Saccades: Overlapping Neural Systems. Neuroimage. 11:210–216.

O'Shea J, Sebastian C, Boorman ED, Johansen-Berg H, Rushworth MFS. 2007. Functional specificity of human premotor-motor cortical interactions during action selection. Eur J Neurosci. 26:2085–2095.

Okamoto M, Dan H, Sakamoto K, Takeo K, Shimizu K, Kohno S, Oda I, Isobe S, Suzuki T, Kohyama K, Dan I. 2004. Three-dimensional probabilistic anatomical cranio-cerebral correlation via the international 10-20 system oriented for transcranial functional brain mapping. Neuroimage. 21:99–111.

Oldfield RC. 1971. The assessment and analysis of handedness: The Edinburgh inventory. Neuropsychologia. 9:97–113.

Ortu E, Ruge D, Deriu F, Rothwell JC. 2009. Theta Burst Stimulation over the human primary motor cortex modulates neural processes involved in movement preparation. Clin Neurophysiol. 120:1195–1203.

Papadourakis V, Raos V. 2018. Neurons in the Macaque Dorsal Premotor Cortex Respond to Execution and Observation of Actions. Cereb Cortex. 1–15.

Passingham RE. 1987. Two cortical systems for directing movement. Ciba Found Symp. 132:151–164.

Passingham RE. 1989. Premotor cortex and the retrieval of movement. Brain Behav Evol. 33:189–192.

Passingham RE. 1993. The frontal lobes and voluntary action, Oxford psychology series, No. 21.

Petrides M. 1985. Deficits in non-spatial conditional associative learning after periarcuate lesions in the monkey. Behav Brain Res. 16:95–101.

Pochon J-B. 2001. The role of dorsolateral prefrontal cortex in the preparation of forthcoming

actions: an fMRI study. Cereb Cortex. 11:260–266.

Praamstra P, Kleine BU, Schnitzler A. 1999. Magnetic stimulation of the dorsal premotor cortex modulates the Simon effect. Neuroreport. 10:3671–3674.

Raos V, Umiltá M-A, Gallese V, Fogassi L. 2004. Functional Properties of Grasping-Related Neurons in the Dorsal Premotor Area F2 of the Macaque Monkey. J Neurophysiol. 92:1990–2002.

Rizzolatti G, Camarda R, Fogassi L, Gentilucci M, Luppino G, Matelli M. 1988. Functional organization of inferior area 6 in the macaque monkey - II. Area F5 and the control of distal movements. Exp Brain Res. 71:491–507.

Rizzolatti G, Cattaneo L, Fabbri-Destro M, Rozzi S. 2014. Cortical mechanisms underlying the organization of goal-directed actions and mirror neuron-based action understanding. Physiol Rev. 94:655–706.

Rizzolatti G, Fadiga L, Gallese V, Fogassi L. 1996. Premotor cortex and the recognition of motor actions. Cogn Brain Res.

Rizzolatti G, Fogassi L, Gallese V. 2002. Motor and cognitive functions of the ventral premotor cortex. Curr Opin Neurobiol.

Rizzolatti G, Luppino G. 2001. The Cortical Motor System. Neuron. 31:889–901.

Rizzolatti G, Matelli M. 2003. Two different streams form the dorsal visual system: Anatomy and functions. In: Experimental Brain Research. p. 146–157.

Rizzolatti G, Scandolara C, Matelli M, Gentilucci M. 1981. Afferent properties of periarcuate neurons in macaque monkeys. II. Visual responses. Behav Brain Res. 2:147–163.

Rossi S, Hallett M, Rossini PM, Pascual-Leone A, Avanzini G, Bestmann S, Berardelli A, Brewer C, Canli T, Cantello R, Chen R, Classen J, Demitrack M, Di Lazzaro V, Epstein CM, George MS, Fregni F, Ilmoniemi R, Jalinous R, Karp B, Lefaucheur JP, Lisanby S, Meunier S, Miniussi C, Miranda P, Padberg F, Paulus W, Peterchev A, Porteri C, Provost M, Quartarone A, Rotenberg A, Rothwell JC, Ruohonen J, Siebner HR, Thut G, Valls-Solé J, Walsh V, Ugawa Y, Zangen A, Ziemann U. 2009. Safety, ethical considerations, and application guidelines for the use of transcranial magnetic stimulation in clinical practice and research. Clin Neurophysiol. 120:2008–2039.

Sakreida K. 2005. Motion class dependency in observers' motor areas revealed by functional magnetic resonance imaging. J Neurosci. 25:1335–1342.

Sallet J, Mars RB, Noonan MP, Neubert F-X, Jbabdi S, O'Reilly JX, Filippini N, Thomas AG, Rushworth MF. 2013. The Organization of Dorsal Frontal Cortex in Humans and Macaques. J Neurosci. 33:12255–12274.

Saur D, Kreher BW, Schnell S, Kümmerer D, Kellmeyer P, Vry M-S, Umarova R, Musso M, Glauche V, Abel S, Huber W, Rijntjes M, Hennig J, Weiller C. 2008. Ventral and dorsal pathways for language. Proc Natl Acad Sci U S A. 105:18035–18040.

Schaffelhofer S, Scherberger H. 2016. Object vision to hand action in macaque parietal, premotor, and motor cortices. Elife. 5.

Schluter N., Krams M, Rushworth MF., Passingham R. 2001. Cerebral dominance for action in the human brain: the selection of actions. Neuropsychologia. 39:105–113.

Schluter ND, Rushworth MFS, Passingham RE, Mills KR. 1998. Temporary interference in human

lateral premotor cortex suggests dominance for the selection of movements. A study using transcranial magnetic stimulation. Brain. 121:785–799.

Schubotz RI, Anwander A, Knösche TR, von Cramon DY, Tittgemeyer M. 2010. Anatomical and functional parcellation of the human lateral premotor cortex. Neuroimage. 50:396–408.

Shannon C. 1949. Communications in the presence of noise. Proc Inst Radio Eng. 37:10–21.

Shen L, Alexander GE. 1997. Preferential representation of instructed target location versus limb trajectory in dorsal premotor area. J Neurophysiol. 77:1195–1212.

Simon JR, Rudell AP. 1967. Auditory S-R compatibility: The effect of an irrelevant cue on information processing. J Appl Psychol. 51:300–304.

Stippich C, Ochmann H, Sartor K. 2002. Somatotopic mapping of the human primary sensorimotor cortex during motor imagery and motor execution by functional magnetic resonance imaging. Neurosci Lett. 331:50–54.

Stoeckel C, Gough PM, Watkins KE, Devlin JT. 2009. Supramarginal gyrus involvement in visual word recognition. Cortex. 45:1091–1096.

Stokes MG, Chambers CD, Gould IC, English T, McNaught E, McDonald O, Mattingley JB. 2007. Distance-adjusted motor threshold for transcranial magnetic stimulation. Clin Neurophysiol. 118:1617–1625.

Tanji J, Okano K, Sato KC. 1988. Neuronal activity in cortical motor areas related to ipsilateral, contralateral, and bilateral digit movements of the monkey. J Neurophysiol. 60:325–343.

Tomassini V, Jbabdi S, Klein JC, Behrens TEJ, Pozzilli C, Matthews PM, Rushworth MFS, Johansen-Berg H. 2007. Diffusion-Weighted Imaging Tractography-Based Parcellation of the Human Lateral Premotor Cortex Identifies Dorsal and Ventral Subregions with Anatomical and Functional Specializations. J Neurosci. 27:10259–10269.

Toni I, Rushworth M, Passingham R. 2001. Neural correlates of visuomotor associations. Exp Brain Res. 141:359–369.

Turella L, Tucciarelli R, Oosterhof NN, Weisz N, Rumiati R, Lingnau A. 2016. Beta band modulations underlie action representations for movement planning. Neuroimage. 136:197–207.

Vargas-Irwin CE, Franquemont L, Black MJ, Donoghue JP. 2015. Linking Objects to Actions: Encoding of Target Object and Grasping Strategy in Primate Ventral Premotor Cortex. J Neurosci. 35:10888–10897.

Verhagen L, Dijkerman HC, Medendorp WP, Toni I. 2012. Cortical Dynamics of Sensorimotor Integration during Grasp Planning. J Neurosci. 32:4508–4519.

Weinrich M, Wise SP. 1982. The premotor cortex of the monkey. J Neurosci. 2:1329–1345.

Wheaton KJ, Thompson JC, Syngeniotis A, Abbott DF, Puce A. 2004. Viewing the motion of human body parts activates different regions of premotor, temporal, and parietal cortex. Neuroimage. 22:277–288.

Wise SP, di Pellegrino G, Boussaoud D. 1996. The premotor cortex and nonstandard sensorimotor mapping. Can J Physiol Pharmacol. 74:469–482.

Zilles K, Schleicher A, Palomero-Gallagher N, Amunts K. 2002. Quantitative analysis of cyto- and receptor architecture of the human brain. In: Brain Mapping: The Methods, J. C. Mazziotta and A. Toga (eds.), USA: Elsevier, 2002, p. 573-602.

Zilles K, Amunts K. 2010. Centenary of Brodmann's map - conception and fate. Nature Reviews Neuroscience 11(2): 119-145.

TABLES

Table 1: *Statistical parameters (t-values) in all conditions of interest for each spot*

	Grid spots									
	1	2	3	4	5	6	7	8	9	10
	Hand / Foot									
Hand	-2,75	-3,28	**-3,92***	-2,67	**-6,66***	**-6,83***	**-3,93***	-3,23	**-4,85***	-0,86
Foot	-1,98	**-4,78***	-1,48	**-4,85***	**-3,62***	-1,86	-2,56	-1,79	-2,45	-0,77
Foot>hand	-0,37	0,32	1,79	-0,15	0,75	**2,49***	0,97	0,79	1,06	0,19
	Hand only - stimulus left / stimulus right									
Left	-1,60	-1,83	-2,34	-1,88	-3,25	**-6,45***	-2,44	-2,05	**-3,90***	-1,70
Right	-1,62	**-3,29***	-2,95	-2,61	**-6,98***	**-4,23***	**-3,77***	-2,16	-2,14	0,43
Right>left	0,17	-1,05	-0,62	-0,81	-1,80	-0,07	0,14	-0,51	0,81	**2,45***
	Hand only - response left / response right									
Left	-1,11	-2,62	-1,57	-3,15	-2,71	**-4,56***	**-3,88***	-1,58	**-6,09***	-0,68
Right	-2,37	-1,91	**-5,66***	-1,87	**-5,67***	**-5,09***	-2,45	**-3,51***	-1,22	-0,66
Right>left	-1,36	-0,19	-1,28	0,24	-1,50	-0,36	0,00	-0,76	**2,26***	0,01
	Foot only – stimulus left / stimulus right									
Left	-2,37	-2,63	-1,89	**-3,80***	-2,84	-2,36	-2,09	-0,68	-1,72	-0,28
Right	-1,10	-2,87	-0,58	-1,36	-2,69	-1,05	-1,52	-2,50	-2,76	-1,14
Right>left	1,49	-0,23	0,87	1,19	0,18	0,95	0,43	-1,69	-0,06	-0,86
	Foot only - response left / response right									
Left	-1,53	-2,21	-0,48	**-3,94***	-3,08	-1,75	-2,65	-2,51	-2,86	-2,05
Right	-1,80	**-4,25***	-1,31	-1,21	-2,26	-1,43	-0,83	-0,56	-0,82	0,29
Right>left	-0,33	-0,68	-0,90	1,17	0,29	-0,05	0,85	1,06	1,07	2,03

Note. * p<.005

Table 2*: Mean RTs (in ms) in each different condition of interest. The standard deviation for each condition is indicated in brackets*

	Grid spots										
	sham	1	2	3	4	5	6	7	8	9	10
	Hand / Foot										
Hand	325 (58)	316 (54)	312 (59)	314 (63)	317 (59)	308 (54)	305 (57)	313 (62)	310 (57)	309 (56)	319 (58)
Foot	406 (90)	386 (66)	394 (81)	400 (96)	393 (71)	392 (74)	401 (83)	390 (72)	394 (81)	407 (107)	406 (90)
	Hand only - stimulus left / stimulus right										
Left	326 (59)	318 (58)	314 (61)	319 (70)	319 (59)	314 (60)	307 (56)	314 (60)	313 (62)	310 (60)	316 (60)
Right	323 (57)	314 (52)	310 (59)	309 (57)	315 (60)	302 (48)	304 (59)	314 (64)	308 (55)	309 (53)	323 (57)
	Hand only - response left / response right										
Left	326 (58)	320 (60)	316 (62)	319 (70)	316 (59)	313 (55)	307 (54)	316 (66)	314 (60)	308 (57)	321 (59)
Right	323 (59)	311 (51)	310 (63)	309 (59)	318 (61)	303 (55)	304 (62)	313 (65)	308 (57)	311 (58)	319 (59)
	Foot only – stimulus left / stimulus right										
Left	409 (95)	385 (64)	397 (75)	398 (100)	393 (80)	393 (74)	399 (83)	390 (68)	402 (76)	406 (109)	412 (102)
Right	404 (87)	388 (70)	392 (87)	401 (95)	394 (66)	391 (75)	403 (86)	391 (80)	388 (90)	409 (107)	396 (79)
	Foot only - response left / response right										
Left	401 (85)	386 (67)	392 (78)	398 (89)	386 (76)	387 (78)	393 (83)	383 (71)	382 (72)	391 (92)	394 (95)
Right	412 (97)	386 (71)	396 (86)	402 (108)	401 (77)	398 (70)	410 (87)	399 (77)	407 (93)	427 (130)	415 (88)

Captions to figures

Figure 1. Schematic representation of the trial sequence in the Simon task. Each trial started with a fixation cross (1000 ms), followed by the stimulus presentation which was visible until the participants' response. An intertrial blank screen (4000 ms) was introduced before a new trial sequence. TMS was delivered time-locked to stimulus presentation, with 2 pulses at +50 ms and +150 ms.

Figure 2. A schematic illustration of the 13 stimulation sites superimposed on a Colin27 template brain. For each participant a 10-point grid was drawn over the left premotor cortex (Brodmann's area 6). The location of the premotor cortex is indicated with the dashed line, as a probabilistic map, marking the borders of all cortical surface with a probability 0.1 of being within BA6. (source: the JuBrain Cytoarchitectonic Atlas available at: https://www.jubrain.fz-juelich.de/apps/cytoviewer/cytoviewer-main.php# (Mohlberg et al. 2012)). The grid (numbered circles) was determined by referencing to the individual motor hand area, motor foot area and motor lip area, which corresponded also to the 3 control sham points (crossed circles). The central sulcus is marked with the solid line.

Figure 3. Individual statistical maps of the t-values obtained contrasting the individual effect of TMS compared to sham stimulation at each of the TMS active spots against the null hypothesis of the mean value = 0. Values of t are reported when they exceeded 3.29, that is, the one corresponding to a P-value of P = 0.005 (t-value Bonferroni-corrected for 10 multiple comparisons) at 15 degrees of freedom. Negative t-values (in blue) indicate shortened RTs, and positive t-values (in red) indicate increased RTs from active TMS compared to sham. Individual maps of t-statistics were grouped according to behavioral factors of interest: 1) Foot responses vs hand responses (A vs. B, upper panel). 2) Left hand responses vs. right hand responses (C vs. D, middle panel). 3) Hand responses to left stimuli vs. hand responses to right stimuli (E vs. F, middle panel). 4) Left foot responses vs. right foot responses (G vs. H, lower panel). 5) Foot responses to left stimuli vs. foot responses to right (I vs. J, lower panel).

Figure 4. Behavioral effect calculated in the sham condition. A. Mean RTs and mean accuracy value, as a function of effector (hand vs. foot) and congruency (congruent vs. incongruent). B. The size of the Simon effect (incongruent minus congruent trials) for RT values and accuracy rates as a function of TMS stimulation sites for hand and foot actions. Error bars represent ±1 SEM.

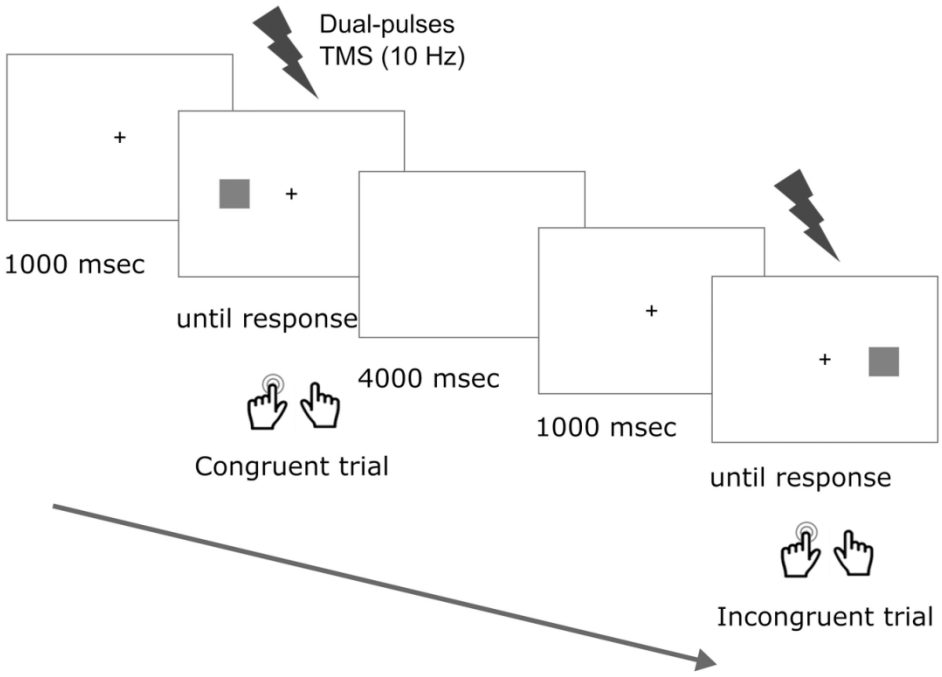

Figure 1. Schematic representation of the trial sequence in the Simon task. Each trial started with a fixation cross (1000 ms), followed by the stimulus presentation which was visible until the participants' response. An intertrial blank screen (4000 ms) was introduced before a new trial sequence. TMS was delivered time-locked to stimulus presentation, with 2 pulses at +50 ms and +150 ms.

120x83mm (300 x 300 DPI)

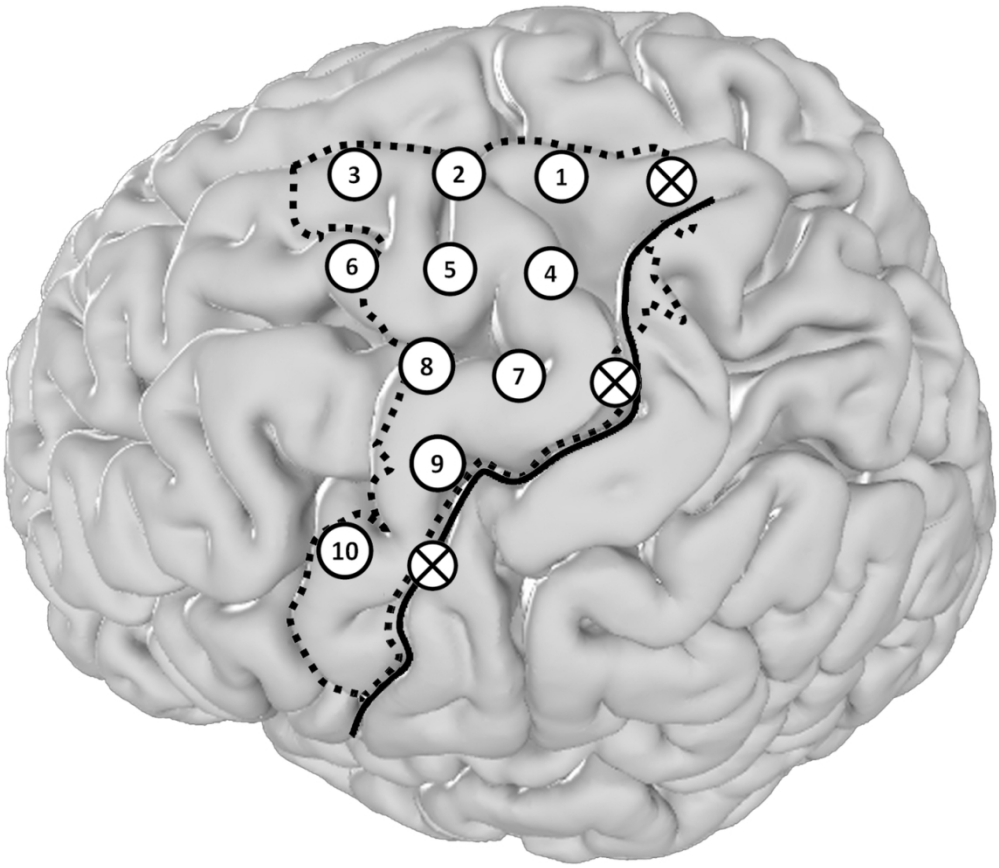

Figure 2. A schematic illustration of the 13 stimulation sites superimposed on a Colin27 template brain. For each participant a 10-point grid was drawn over the left premotor cortex (Brodmann's area 6). The location of the premotor cortex is indicated with the dashed line, as a probabilistic map, marking the borders of all cortical surface with a probability 0.1 of being within BA6. (source: the JuBrain Cytoarchitectonic Atlas available at: https://www.jubrain.fz-juelich.de/apps/cytoviewer/cytoviewer-main.php# (Mohlberg et al. 2012)). The grid (numbered circles) was determined by referencing to the individual motor hand area, motor foot area and motor lip area, which corresponded also to the 3 control sham points (crossed circles). The central sulcus is marked with the solid line.

119x103mm (300 x 300 DPI)

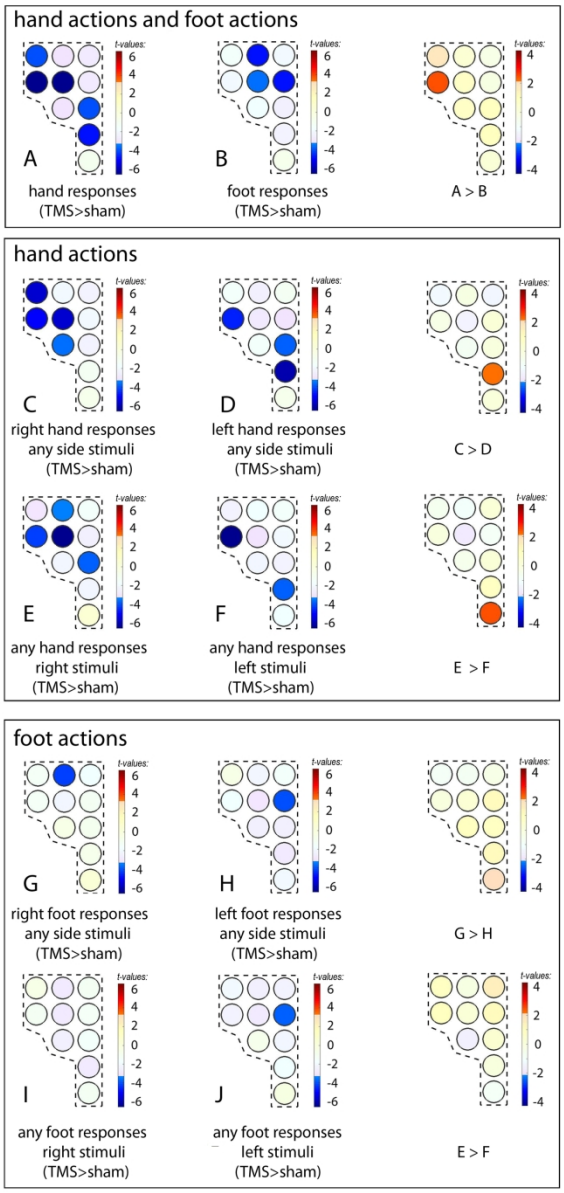

Figure 3. Individual statistical maps of the t-values obtained contrasting the individual effect of TMS compared to sham stimulation at each of the TMS active spots against the null hypothesis of the mean value = 0. Values of t are reported when they exceeded 3.29, that is, the one corresponding to a P-value of P = 0.005 (t-value Bonferroni-corrected for 10 multiple comparisons) at 15 degrees of freedom. Negative t-values (in blue) indicate shortened RTs, and positive t-values (in red) indicate increased RTs from active TMS compared to sham. Individual maps of t-statistics were grouped according to behavioral factors of interest: 1) Foot responses vs hand responses (A vs. B, upper panel). 2) Left hand responses vs. right hand responses (C vs. D, middle panel). 3) Hand responses to left stimuli vs. hand responses to right stimuli (E vs. F, middle panel). 4) Left foot responses vs. right foot responses (G vs. H, lower panel). 5) Foot responses to left stimuli vs. foot responses to right (I vs. J, lower panel).

122x256mm (300 x 300 DPI)

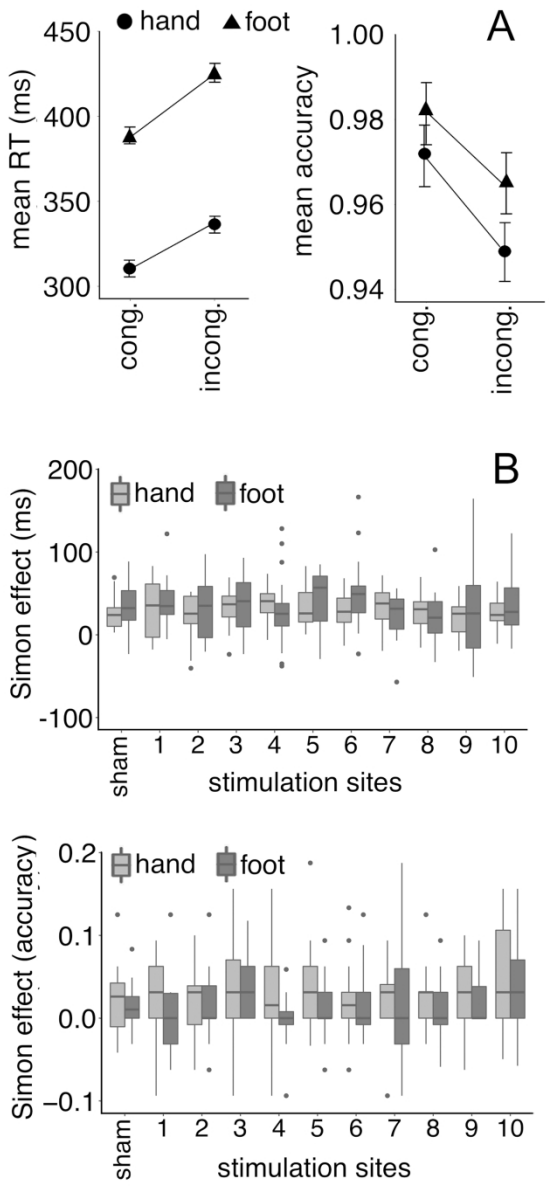

Figure 4. Behavioral effect calculated in the sham condition. A. Mean RTs and mean accuracy value, as a function of effector (hand vs. foot) and congruency (congruent vs. incongruent). B. The size of the Simon effect (incongruent minus congruent trials) for RT values and accuracy rates as a function of TMS stimulation sites for hand and foot actions. Error bars represent ±1 SEM.

119x257mm (300 x 300 DPI)